Title
STUDIES OF THE VAPORIZATION MECHANISM OF ICE SINGLE CRYSTALS

Authors
Davy, J. Gordon
Somorjai, G.A.

Publication Date
1971-03-01

Submitted to Journal
of Chemical Physics

UCRL-20530
Preprint

STUDIES OF THE VAPORIZATION MECHANISM OF ICE SINGLE CRYSTALS

J. Gordon Davy and G. A. Somorjai

March 1971

AEC Contract No. W-7405-eng-48

LAWRENCE RADIATION LABORATORY
UNIVERSITY of CALIFORNIA BERKELEY

UCRL-20530

DISCLAIMER

STUDIES OF THE VAPORIZATION MECHANISM OF ICE SINGLE CRYSTALS†

J. Gordon Davy* and G. A. Somorjai

Inorganic Materials Research Division,
Lawrence Radiation Laboratory
and
The Department of Chemistry,
University of California,
Berkeley, California

ABSTRACT

The kinetics of the vacuum sublimation of ice single crystals has been investigated by a vacuum microbalance technique in the temperature range -90° to -40°C. The vaporization coefficient a_v = (observed vaporization rate) ÷ (theoretical maximum rate) and the activation enthalpy of sublimation, ΔH_s^*, vary markedly with temperature in this range. At temperatures below about -85°C, $a_v = 1$ and ΔH_s^* equals the thermodynamic enthalpy of sublimation ΔH_s°. Between about -85° and -60°C, a_v decreases slowly with increasing temperature, $\Delta H_s^* \lesssim \Delta H_s^\circ$. Between about -60° and -40°C, a_v decreases progressively more rapidly with increasing temperature and ΔH_s^* decreases to a high-temperature limiting value of $\simeq \frac{1}{2}\Delta H_s^\circ$. The effects of various experimental parameters such as crystal orientation, doping with impurities and adsorbed gases on the ice vaporization kinetics have also been investigated. Neither grain boundaries nor crystalline orientation has a measurable effect on the rate. Ice doped with monovalent impurities was found to vaporize at steady-state rates that were uniformly lower over the entire temperature range of the study. Also, NH_3 (gas) and HF (gas), present in the ambient at pressures $\sim 10^{-3}$ to 10^{-2} torr, reduce and increase respectively, the ice vaporization rate.

* Present address: RCA David Sarnoff Research Center, Princeton, New Jersey.

† Based on the Ph.D. Thesis by J. G. Davy presented to the University of California, Berkeley, California 94720.

The experimental results, along with previously reported physical-chemical properties of ice are used to arrive at a vaporization mechanism: Ice at equilibrium with the vapor has a surface population of a highly mobile species assumed to be water molecules hydrogen-bonded to only one nearest neighbor. These energetic molecules are the source of the vapor flux leaving the surface. At sufficiently low temperatures, vacuum vaporization does not occur rapidly enough to alter this equilibrium surface population. Sublimation at higher temperatures however, depletes the population to a progressively greater extent with increasing temperature. Thus the rate limiting step in vaporization, which is the <u>desorption</u> of the mobile water molecules at low temperatures, changes to their <u>formation</u> at high temperatures.

INTRODUCTION

A thorough study of the evaporation kinetics, along with other physical-chemical properties of a solid or liquid, may be used to arrive at a sequence of steps or mechanism by which molecules from the condensed phase enter into the vapor phase. Although the vaporization rates for many materials have been measured, vaporization mechanisms have been proposed for only a few, due to the lack of more detailed kinetic information. Thus, the vaporization rate of (polycrystalline) ice has been previously measured by several researchers but none has suggested a mechanism. Ice is a material of great importance in our environment and it is of interest both in its own right and as a prototype of hydrogen-bonded compounds.

We have studied the vaporization of ice crystal surfaces (the ordinary hexagonal modification, commonly called ice I) into vacuum (free or Langmuir vaporization) over a temperature range -90°C to -40°C. The effects of a) crystallinity and crystal orientation, and b) various impurities in the crystal lattice and the influence of different gases over the vaporizing surface on the evaporation rates were also investigated. In this paper we report the results of these investigations and propose a vaporization mechanism that is consistent with the experimental findings and with other known properties of ice.

The theoretical maximum possible rate of vaporization $J_{max}(T)$ can be computed from the equilibrium vapor pressure P_{eq} of the solid according to the equation,

$$J_{max}\left(\frac{\text{mole}}{\text{cm}^2\text{sec}}\right) = P_{eq}\,(2\pi MRT)^{-\frac{1}{2}}$$

since in equilibrium the condensation and vaporization rates are identical. Here M is the molecular weight of the vapor molecules and R and T have their usual meaning. It is customary to define a vaporization coefficient, $\alpha_v(T)$, as $\alpha_v(T) = \frac{J(T)}{J_{max}(T)}$. Its magnitude is a measure of the departure of the actual vaporization rate from the theoretical maximum. By a Clausius-Clapeyron treatment, it may be shown that a plot of log J_{max} vs. T^{-1} gives a line whose slope is $\frac{-\Delta H_s^\circ}{2.3R} + \frac{T}{4.6}$, where ΔH_s° is the equilibrium enthalpy of sublimation. The second term is always less than 5% of the first and if it is ignored the slope can be taken to give ΔH_s° directly. If instead log J vs. T^{-1} is plotted, the slope can be taken to give a corresponding parameter ΔH_s^*: the activation enthalpy of sublimation. A more detailed discussion of the various vaporization parameters is reported elsewhere.[1]

We have found that both the activation enthalpy of sublimation and the vaporization coefficient for high purity ice decreases markedly with increasing temperature in the range -90° to -40°C. At temperatures below -85°C, $\Delta H_s^* = \Delta H_s^\circ$ and $\alpha_v = 1$. Toward -40°C ΔH_s^* decreases to a high-temperature value $\Delta H_s^* \simeq \frac{1}{2}\Delta H_s^\circ$ and α_v is already less than 0.4 at 45°C. The vaporization mechanism of ice changes in our temperature range of study. It appears that at low temperatures (< -80°C) the rate-limiting step in the vaporization of ice is the desorption of water molecules, while at high temperatures (> -40°) the rate-limiting step is the formation at the surface of water molecules that are held by one hydrogen bond.

SELECTED PHYSICAL-CHEMICAL PROPERTIES OF ICE

The literature available on ice is voluminous and covers a wide range of topics, including glaciology and reports on the suitability of ice for airplane runways. Out of this wealth of information we will review only those physical-chemical properties of ice which will be of importance in our attempt to interpret the mechanism of ice vaporization. Where possible in this section, references are given to review articles.

Vapor Pressure. The saturation vapor pressure of ice is best known at the triple point: $T_o = 273.16°K$, $P_o = 4.58$ torr. The standard enthalpies of sublimation at the triplet point and at absolute zero are given by Eisenberg and Kauzmann;[2] $\Delta H_s^\circ = 12{,}203$ and $11{,}317$ kcal mole^{-1} respectively.

A thorough evaluation of the ice vapor pressure, based on both experimental measurements and on thermodynamic calculations has been made recently by Jancso, Pupezin and Van Hook.[3] The most extensive tabulation of the saturation vapor pressure of ice is contained in the Smithsonian Meteorological Tables.[4] Use of these tables make calculations from analytical expressions rarely, if ever, necessary.

Previous Measurements of Ice Vaporization Rates. The results of all previous investigations of the vaporization rate of (polycrystalline) ice is given in Figure 1, along with the results of the present study. Except as noted the ice samples used by these workers were prepared by degassing and then freezing distilled water under vacuum just prior to performing their measurements.

Delaney et al.,[5] used a non-steady-state technique to obtain a value $\alpha_v = 0.0144 \pm .0020$ for temperatures between -13° and -2°C, and for an incident flux J_i nearly equal to the departing flux J_d, i.e., $J_i/J_d \lesssim 1$.

The two lines marked D in Figure 1 were obtained by plotting values of $\alpha_v J_{max}$ for the two runs they report. Note that the predicted rates at these temperatures are near those observed between -50° and -40°C. However, since α_v may depend on J_i/J_d, it is not certain that these results are directly comparable to the results from free vaporization studies (i.e., $J_i/J_d \ll 1$).

Baranaev[6] used the method of Alty[7] to obtain the vaporization rate at -48°, -46°, and -44°C. A straight line fitted to these values is marked B in Figure 4. Although Baranaev calculated his results assuming that $J_i \ll J_d$, the low values ($\bar{\alpha}_v = 0.068$) obtained make his assumption doubtful. Another possibility is that the temperature measurements were in error due to thermal gradients in the sample. Baranaev does not state whether the water from which he froze his sample had been degassed.

Strickland-Constable and Bruce[8] used a balance technique with a liquid-air cooled condenser subtending part of the solid angle above the vaporizing surface. Apparently they did not degas their water prior to freezing. Their results, for -55° to -50°C, are shown by the line labeled SCB. These workers considered gas-phase collisions and suggest that $\alpha_v = 1$.

Kramers and Stemerding[9] also used a balance technique and a plane-parallel condenser, which they positioned at distances between 13 and 44 mm from the vaporizing surface. They experienced difficulty maintaining a uniform surface temperature. Because of the large scatter of their results -- α_v between 0.5 and 1.4--only their temperature range (-60° to -40°C) is indicated (between arrows marked KS). For these studies, the condenser temperature was never more than 12°C below the temperature of the vaporizing surface. This resulted in a non-negligible flux incident on the vaporizing surface, which they took into account. Within the accuracy of their results there was no apparent tendency for the incident flux to lower α ;

in fact they concluded that $\alpha_v = 1$ over their temperature range and that departures of J below the calculated rate were due to gas-phase collisions and wall effects.

Tschudin[10] used an electrical balance and a liquid-air cooled condenser positioned a few millimeters over the vaporizing surface. After making 43 rate measurements between -85°C and -60°C, he concluded that $\alpha_v = 0.94 \pm 0.06$ over the temperature range (shown in Figure 4 between arrows marked Ts).

Koros et al.[11] measured the condensation coefficient of water molecules on ice using a molecular beam apparatus. In the temperature range -140° to -115°C, they report a value for α_c of 0.83 ± 0.15. Because these results are for condensation rather than vaporization, they are not shown.

Isono and Iwai[12] measured a condensation coefficient of about 0.06 between -50° and -80°C; below this temperature they observed that the condensation coefficient increases to about 0.5 at -110°C.

Association of Water Molecules in the Vapor. In our consideration of ice vaporization the possibility of the presence of water molecule polymers such as the dimer $(H_2O)_2$ in the vapor has been ignored.

Eisenberg and Kauzmann[2] review various attempts to calculate the dimer concentration in water vapor. A dimer/monomer molecular ratio of only about 5×10^{-4} may be estimated at 0°C. More recently, Milne and Greene[13] and Greene et al.[14] have carried out mass-spectrometric sampling of near-saturated water vapor, obtaining a dimer/monomer ratio varying between 3×10^{-4} at 0°C and 1.6×10^{-2} at 100°C. No measurements of the dimer concentration in water vapor at temperatures below 0°C have been reported. While it is possible that the dimer/monomer ratio for free vaporization

of ice is somewhat different than for saturated water vapor, it would need to be at least two orders of magnitude higher in order to be an important feature in the vaporization kinetics.

The Morphology of the Ice Surface. The nature of the ice surface has been the subject of active interest since the time of Faraday, who in 1850 proposed that ice at temperatures near the melting point was covered by a liquid-like film. The bibliography now available on this one topic alone is long, and we mention here only the review by Jellinek.[15] The liquid-like film was postulated to explain the ease with which two pieces of ice stick together. This property was termed "regelation" by Tyndall, but is now explained as sintering. This sintering is attributable to surface molecules of high surface mobility, and occurs at measurable speed down to -25°C or below in a water-saturated atmosphere, but only to -3°C in a dry atmosphere. For present purposes, this is one of the more important characteristics of the ice surface: the population of the highly mobile species (liquid-like or other) is observed to be greatly reduced under dry (high net vaporization) conditions.

An electron microscope study of the subliming ice surface has been published recently.[16] One of the conclusions that could be drawn from this study was that the ice surface becomes progressively rougher with increasing temperature above -90°C.

Structure[17] and Lattice Defects[18] of Ice. Under ordinary pressures ice has a hexagonal crystal structure commonly called ice I. The structure of the oxygen sublattice of ice I was determined by Bragg in 1922 to be that of würtzite, but the positions of the hydrogen atoms were in question until 1957, when they were determined by neutron diffraction of D_2O ice. Each oxygen atom has two hydrogen atoms attached to it along the

oxygen-oxygen directions at a distance of 0.99 Å, and is tetrahedrally surrounded by four oxygen atoms. In ice all the HOH bond angles are very near the tetrahedral angle of $109\frac{1}{2}°$. Upon vaporization the bond angle for the vapor molecule changes to 105°.

A cubic form of ice (I_c) has also been prepared by depositing water vapor on a cold substrate. The cubic modification transforms into hexagonal ice I_h structure upon warming above about -100°C.

Much has been written about defects in the lattice of real ice, but there remain substantial uncertainties about each of the various types. Dislocations, which play a central role in ice mechanical properties, are known to exist in unstrained ice in very low concentrations, but quantitative estimates vary widely (~ 1 cm^{-2}, Webb and Hayes[19]; $\sim 10^4$ cm^{-2}; Fukuda and Higashi[20]). Although dislocations are known to influence the vaporization rate of NaCl,[21] we could find no effect attributable to them in ice vaporization.

The most thoroughly studied ice defects are those first described in 1951 by Bjerrum: ionic (H_3O^+ and HO^-) and orientational (L and D, described in more detail below). These defects account for the observed dc and ac electrical properties of ice. A series of three papers by A. Von Hippel and co-workers[22] that appeared recently has shown that many previous measurements of these properties have been subject to great uncertainty, and reported values are often artifacts of the measuring technique. As a result, values for the concentrations, mobilities, and activation energies for ionic and orientational defects, particularly at the temperatures of present interest, must be considered as uncertain.

Nevertheless, it should be possible to make some qualitative comments. The concentration of all point defects in pure ice even close to the melting

point is certainly very small (for example, von Hippel et al.[22] estimate the ion concentration at -4° to be about 3×10^{11} cm^{-3}). It seems reasonable that unless defects were in some way directly involved with the vaporization of each molecule, their effect would be too small to be observable.

The number of defects in ice should in principle be alterable by doping.[23] The total ion concentration in ice doped with strong acids and bases remains small, however, both because of their low solubilities and their low ionization constants in ice.[24] Orientational defects on the other hand can be introduced more readily by doping. In pure ice, these defects are formed by an intramolecular proton jump between bonds (as opposed to the intermolecular proton jump along a bond which creates an ion pair). Thus an L-defect is an oxygen-oxygen bridge without a proton; a D-defect is a bridge with two protons. The D-L defect pair creation step may also be thought of as a molecular rotation; further rotations can separate the defects (or annihilate them) and once separated they can migrate independently through the crystal lattice.

Orientational defect concentrations can be altered appreciably by suitable doping: each HF or NH_3 molecule substituted on an H_2O site introduces an L- or D-defect.[23] Jones and Glen[25] found that ice doped with HF in concentrations up to 67 ppm was softer than pure ice, while ice doped with NH_3 appeared to be harder than pure ice. They attribute the softening to the formation of excess L-defects, and suggested that D-defects did not cause softening either because D-defects produced by NH_3 were not mobile (trapped by NH_3), or because D-defects were immobilized by dislocations. If D-defects are not mobile and cannot cause softening in the manner of L-defects, then the net result of NH_3 doping is a reduction in the mobile

L-defects concentration below the pure ice value and subsequent hardening. The literature on the role of impurities in the ice lattice is extensive. The impurities produce a variety of effects (even at very low concentrations) many of which are only partially understood. For a recent thorough review, see Gross.[23]

Since bonding in ice is predominantly by hydrogen bonds it is not surprising that a variety of physical-chemical phenomena, such as sublimation, self-diffusion, dielectric relaxation, etc., require activation energies close to that required to break one or more hydrogen bonds. In fact, the activation energies of different molecular processes in the ice lattice should be predictable after taking account the lattice relaxation energy about the molecule with broken hydrogen bonds. An excellent review of lattice defects, of various lattice processes and their mechanisms, and their relationship with the hydrogen-bond energy, is given by Onsager and Runnels.[26]

EXPERIMENTAL

Sample Preparation. For vacuum vaporization it is desirable to use single crystals of known orientation, at least until it can be demonstrated that neither orientation nor the presence of grain boundaries affect the observed vaporization rate of ice. The method employed by Jona and Scherrer[27] was used to prepare single crystals of ice for most of our vaporization studies. The ice crystal growth was carried out in a walk-in freezer maintained at -10°C.

Large pieces of very clear ice are obtained from distilled water by slow growth in a 600 ml beaker. Because ice is transparent and optically active, a suitable single-crystalline region can be readily selected using polarized light and cutting away from its neighbors with a hot wire. The orientation of the

crystal is determined in a polarizing microscope.[28] The desired sample has one exposed face of known surface area, so an aluminum sleeve (5/16" dia., 1/4" long, 0.005" wall thickness) is melted down into the ice and the excess is trimmed away with a knife. A small thermocouple (0.003" copper-constantan) is "welded" to the back face of the crystal with a few drops of water and then this face is covered. The finished sample is then ready to be suspended from the microbalance.

The same growth technique was used to prepare "doped" ice samples: ice was grown from 0.1M and 0.01M solutions of NH_4OH, LiOH, NaOH, HF, HNO_3, NH_4F, LiF and NaF to cause their incorporation into the ice lattice in order to investigate the influence of these impurities on the vaporation rate.

It is remarkable that while water is an excellent solvent, the solubility of all these materials in ice, with the exception of NH_4F, is on the order of parts per million or less.[23] NH_4F, which is isoelectronic with two H_2O molecules and has the same crystal structure as ice has a solubility in ice of 7 mole percent at the eutectic temperature of -28°C.[29] However, large, clear single crystals of NH_4F-doped ice are obtainable only for concentrations below about 0.1 mole percent; for NH_4OH and HF the solubility limit is about 0.01 mole percent ($\approx$ 100 ppm).[30] The solubility of most other dopants is unknown, but they are likely to be very low: HCl and NaOH dissolve only to about 0.1 ppm.[24] For purposes of this discussion, the ice grown by the Jona-Scherrer method from distilled water will be called undoped. As another method of preparing ice (clear, but polycrystalline, with a grain size ~ 1 mm), distilled water with a conductivity below 10^{-6} $(ohm\text{-}cm)^{-1}$ was degassed under vacuum for several hours. Then the degassed water was frozen still (under vacuum) at

a rate of about 10 μ/sec. These samples we call high-purity, because it is possible to keep their total contaminant level lower than in the so-called undoped samples.

Vaporization System. A diagram of the microbalance system used to measure the vaporization rate, J, of ice is shown in Figure 2a. Both the weight-loss and the rate may be continuously monitored as a function of time by electronically taking the time derivative of the sample weight change measured by the microbalance. The measured noise levels are: balance, ± 1 μg; differentiator, ± 1 μg/min. Estimated errors for both balance and differentiator measurements are on the order of 1%. The microbalance and differentiator are described in detail elsewhere.[31] Thus with this microbalance system it is possible to obtain accurate absolute weight-loss or rate measurements continuously and the sample temperature can be monitored simultaneously.

In order to install the sample in the vacuum chamber without haste, we found it helpful to first insert a miniature cold chamber to partially surround the ice sample and keep it from melting while the thermocouple leads were connected and the sample was suspended from the balance arm. The cold chamber has two compartments: one for the sample and one which is filled with a dry-ice acetone slurry. It was removed from the vacuum chamber just prior to pumpdown.

Once evacuation of the chamber has started, it takes less than five minutes to reach a steady-state pressure and sample temperature; from that time on it is possible to obtain vaporization rates. The sample is thermally isolated in vacuum as indicated by Figure 2b.

When the vacuum chamber walls are at room temperature, an ice sample's steady-state temperature is about -68°C. For lower temperatures, most of the chamber walls can be chilled by liquid nitrogen within about 15 minutes. The lowest ice sample temperature attainable in the cold vacuum chamber is about -90°C. ¶Since surface cooling gives a vaporization rate too low for the indicated temperature it is important (especially at higher rates of vaporization) that the true surface temperature be known. From the heat balance between the heat loss by sublimation and radiative heat input one can estimate a temperature difference of at most 0.1°C between the vaporizing front and the covered backside of the sample where the thermocouple is located. In order to eliminate possible surface cooling, heat is supplied radiantly to the same surface that is losing it by vaporization as shown in Figure 2b. Thus, under steady-state vaporization conditions, temperature gradients within the solid should not be expected to occur. The radiant heater is a small coil of nichrome wire. The heater control is a high-gain proportional controller capable of maintaining the sample temperature constant to within 0.01°C. The power (heat input) required to maintain the 0.5 cm^2 of ice surface at -70°C, -60°C, -50°C and -40°C assuming $J = J_{max}$ 43, 170, 660 and 2000 milliwatts respectively.

The lowest sample temperature attainable depends primarily on the success in shielding the sample from warm (room-temperature) surroundings. The high-temperature limit is set by success in supplying adequate radiant power to the sample surface. It must also be possible to make a steady-state rate measurement before the surface recedes far into the sleeve,

since reflection of water molecules from the holder walls will modify the observed vaporization rates. Finally, it was observed that at the highest rates obtained ($\sim$ 35 mg cm^{-2} min^{-1}) the sample began to swing due to the sizeable momentum transfer occurring at the vaporizing surface. For the system described here, these difficulties restricted the measurements to temperatures not higher than about -40°C.

When the chamber is warm (room temperature), the ambient pressure of water vapor is measured to be negligible compared to the effective saturation vapor pressure over the accessible temperature range; that is, the flux of water molecules incident upon the surface is small compared to the flux leaving the surface so that condensation effects need not be considered. When the chamber is cold, the ambient pressure is $\sim 10^{-6}$ torr, and the partial pressure of water vapor is presumably much smaller than this.

For investigating the effects of ambient gases on the evaporation rate of ice it is desirable to introduce a gas into an isolated chamber to some arbitrary pressure and have that pressure remain reasonably fixed; this is readily accomplished by having the vacuum chamber walls cold. The walls act as an effective cryopump for water vapor and the background pressure rises at a negligible rate. Even for condensible gases such as HF and NH_3, the partial pressure remains fairly constant in the cold chamber, presumably because these gases first condense and then slowly desorb from warmer regions of the wall area.

RESULTS

Vaporization Rates of Undoped and High Purity Crystals. The time required to reach a steady-state temperature and vaporization rate depends on the temperature, but is on the order of thirty seconds to a few minutes. (Cooling to very low temperatures takes somewhat longer: ~ ½ hr. from -75° to 80°). Consequently, a large number of rate measurements can be carried out on a single sample in a matter of hours. (For some warm-chamber measurements, over a dozen experimental points may be obtained in less than thirty minutes). We have found that for all of the ice samples studied the rate is a function only of temperature, and not of the thermal history or of the amount of sample vaporized. Even for large temperature changes, the observed rates become constant at the same time as the temperature. On the basis of electron micrographs of the vaporizing ice surface[16] it appears that the surface morphology that gives the steady-state rate develops by the time 1000A (~ 300 molecular layers) have sublimed, independent of temperature.

For each ice sample, the values of J, when plotted as the logarithm of J vs T^{-1}, all lie quite accurately on a smooth curve. The evaporation rates of a typical undoped and a typical degassed high purity ice sample as a function of temperature are shown in Figure 3a and 3b, respectively. The uncertainty in the points in these figures is much smaller than the circles used to represent them. Each point represents a separate determination of the steady-state vaporization rate; the numbers give the order in which they were taken. The curves are drawn somewhat above the high-temperature points; a correction was made for the reflection of molecules from the exposed holder walls due to the recession of the ice surface.

The results for five samples each of high-purity and of undoped ice

are shown in Figures 3c-d. The points shown are the averaged rates for five samples, in increments of 10^{-4} in T^{-1}. The bars indicate the spread between the highest and lowest rates observed. The line which would be obtained if the ice vaporized with a maximum rate is shown for comparison. The general shape of the vaporization curve is maintained for all samples including the doped samples (to be discussed below) with the exception of those doped with high concentrations of ammonia and ammonium fluoride, which will be discussed separately. The average vaporization rate for undoped ice is about 10% lower than for high-purity ice (see Figure 3c); the rate for ice of even higher purity might be slightly higher.

For a given sample, the vaporization rate at steady state fluctuates about an average value. The magnitude of this fluctuation is small for the high-purity and the doped samples ($\leq \pm 5$ μg $cm^{-2}min^{-1}$) and large for the undoped samples ($\sim \pm 50$ μg $cm^{-2}min^{-1}$) and is independent of temperature. The fluctuation appears to be due to local variations in impurity content and will be discussed later.

There is a spread in observed vaporization rates from sample to sample for samples of the same type. For degassed high-purity samples, the spread between the highest and lowest rates observed at a given temperature is about 10%; for undoped samples, about 15%.

At low temperatures the vacuum evaporation rates of degassed high-purity ice samples approach the maximum vaporization rate $J_{max}(T)$. Undoped crystals yield rates at low temperatures that are somewhat below the maximum rate ($\alpha_v \sim 0.9$). Nevertheless, below -75°C the activation enthalpy of sublimation, ΔH_s^* is equal to the equilibrium enthalpy of sublimation, $\Delta H_s^* = \Delta H_s^\circ = 12.2$ kcal/mole within the accuracy of the

experiments. At higher temperatures the vacuum vaporization rate of ice falls progressively below the maximum rates. The activation enthalpy of sublimation ΔH_s^* decreases with increasing temperature, asymptotically approaching a value that corresponds to $\frac{1}{2}\Delta H_s^\circ = 6.1$ kcal/mole. In Figure 3d the corresponding variation of the vaporization coefficient α_v with increasing temperature is also displayed.

Effect of Crystal Orientation and Grain Boundaries. The exposed vaporizing surface for all five undoped samples reported in Figures 3c and 3d was the c-face (c-axis normal to the surface). Undoped samples that had other orientations (including c-axis parallel to surface) all had vaporization rates that fell within the sample-to-sample variation for c-face crystals. Also, polycrystalline, undoped samples had vaporization rates indistinguishable from those for the single crystals. Observation by optical microscope of the surface after vaporization (and subsequent exposure to air) showed, for all samples, macroscopically flat but roughened surfaces. The polycrystalline samples showed no evidence of grain-boundary grooving.

Effect of Surface Roughness. In every case, the vacuum evaporation rate, J, is calculated from the observed weight loss and the geometrical or projected surface area of the vaporizing sample. The electron microscope study by Davy and Branton[16] has shown that the surface of a vaporizing ice crystal is relatively smooth while vaporizing at low temperatures ($< -85°C$ for which $\alpha_v = 1$), and that the surface becomes increasingly rough at temperatures $> -85°C$ (for which $\alpha_v < 1$). Since many materials develop a rough surface during vaporization it is necessary to consider the effect of surface roughness on J

when the true surface area exceeds the projected area. It might be expected that a sample with a rough surface may vaporize more rapidly than one with a smooth surface, but the following points are important to consider:

(a) If $\alpha_v = 1$, the vaporization rate per unit of projected area is entirely independent of true surface area. This follows from the thermodynamic condition that the flux across any plane cannot exceed the flux corresponding to the saturation vapor pressure. Melville[32] shows that if $\alpha_v = 1$, the initially larger flux from a rough surface is reduced to the smooth-surface value because molecules vaporizing from one part of the surface can strike another part of the surface and recondense.

(b) Only in the limit of a zero condensation coefficient does the vaporization rate become proportional to the true surface area. This limit is approached by arsenic and phosphorus, as discussed by Brewer and Kane,[33] and by Rosenblatt.[34]

(c) For a single crystal face, the surface area of the vaporizing sample may not be an independent variable. That is, a sample with an initially smooth face may become rough and a sample with an artifically roughened surface may become smoother, and J may not take on a steady value until this occurs.

(d) The increase in true surface area observed on most evaporating single crystals, even those that become quite rough, is probably less than a factor of two over the projected area, and it may be asserted that J takes on an intermediate value between J (flat surface) and J_{max}. In sum, the lack of knowledge of true surface area is often not as serious as it might seem.

Effect of Impurities in the Ice Crystal Lattice on the Vaporization Rate. The vacuum vaporization rates of the doped ice crystals listed above were investigated in order to determine the effect of these impurities on the evaporation kinetics.

Plots of the logarithm of the evaporation rate vs T^{-1} for doped samples have the same appearance as those for undoped samples. There was however, a general overall reduction in the vaporization rate. The results for a number of monovalent impurities are summarized in Table I which gives the values for the vaporization coefficient, $\alpha_v = J_{doped}/J_{max}$, evaluated at -65°C. The effect of one trivalent impurity was investigated; the vaporization rate of ice grown from a saturated solution of $Cr(NO_3)_3$ was measured. The vaporization behavior was indistinguishable from that of an undoped sample and there was no suppression of the rate fluctuation mentioned above.

The results for ice doped with NH_4F differed from those for other dopants; a rate plot for several such samples is given in Figure 4. Since NH_4F is much more soluble in ice than other materials are, it is not surprising that its effect on reducing the ice vaporization rate is more pronounced: α_v for ice grown from 1M NH_4F solution is about 0.06; the activation enthalpy is somewhat above the thermodynamic enthalpy of sublimation.

Of special interest is the behavior of the sample from 1M NH_4OH, which was quick-frozen over dry ice. The result was a slush of small ice grains coated with aqueous ammonia (eutectic temperature -120°C). When this sample was placed in the vaporization chamber, its first vaporization rate values were well above J_{max} due to rapid vaporization of excess ammonia. It eventually reached a steady-state rate with $\alpha_v \sim 0.9$ over the temperature range investigated up to -50°C). The vacuum

vaporization rates of doped ice samples were independent of time, i.e., there was no indication of any time-dependent accumulation of impurities at the vaporizing surface. Thus, due to their low solubilities, the surface concentration of impurities should always be much smaller than the surface concentration of vaporizing water molecules.

Effect of Gases on Ice Vaporization Rate. The influence of the following gases on J was investigated: H_2, He, N_2, O_2, CO_2, $C_2H_2F_4$ (Freon 114), C_2F_6 (Freon 116), H_2S, NH_3, HCl and HF. The gas was admitted to a pressure of about 10^{-3} torr while the temperature of the ice sample was such that its saturation vapor pressure was about 5×10^{-3} torr. Thus, the vaporization flux and the gas flux incident on the surface were of similar magnitude.

All of these gases except NH_3, HCl and HF caused a slight decrease in the vaporization rate attributable to gas-phase collisions near the vaporizing surface.

The effect of NH_3 was a considerably greater reduction in the vaporization rate. HCl did not decrease the rate below the evaporation rate in the vacuum, and HF increased the evaporation rate.

These three gases and N_2 as a reference gas were investigated further to find the temperature and pressure dependence of J_{gas}/J and the results are given in Figure 5a and 5b.

Effect of Collisions Between Vapor Molecules. In most discussions of vaporization, it is assumed that the mean free path for the vaporizing molecules is large compared to the size of the vaporizing surface, and that none of the molecules which leave return as a result of collisions. At high vaporization rates this condition is no longer met: if a parameter β is defined[35] as that fraction which does escape, then $(1-\beta)$ is the fraction of molecules which after their last collision return to the vaporizing surface. By the law of conservation of momentum, this fraction cannot exceed $\frac{1}{2}$, and for colliding molecules with a net momentum away from the surface, the returning fraction will be less than $\frac{1}{2}$, so that β varies only from unity at low vaporization rates, to a minimum value greater than $\frac{1}{2}$ at high rates.

Since high vaporization rates occur in the present study, it is of interest to consider the qualitative influence of gas-phase collisions near the vaporizing surface. Using as worst-case estimates the calculated mean free path of molecules in the equilibrium water vapor, and a minimum β of $\frac{1}{2}$, and assuming a hypothetical $\alpha_v = 1$ over the entire temperature range, it is possible to plot the influence of a diminishing mean free path and β on the vaporization rate of ice samples with a diameter of a few millimeters (Fig. 6). Note that gas-phase collisions have no influence on ΔH_s^* in the high and low limits of β, and have only a small effect for intermediate values. Since the high-rate limiting value for ΔH_s^* actually observed for ice is much less than ΔH_s°, the lowering of the observed α_v cannot be entirely attributed to gas-phase collisions. The true α_v may be somewhat higher, but the influence of collisions (which lowers α_v) is offset by surface roughening (which raises α_v). Moreover, in the case of the 1M NH_4OH sample a constant α_v was observed up to very high rates. Had either surface

cooling or gas-phase collisions been important effects, the pronounced curvature that was exhibited in the rate plots of all other samples would have been seen for this sample as well.

DISCUSSION

The following statements summarize the experimental observations which may be of value in determining the vaporization mechanism of ice single crystals.

1) The vacuum sublimation rate of undoped and high-purity ice has been measured in the temperature range of -90° to -40°C. The sublimation rates of the

different samples were reproducible within ± 10% and were not dependent on crystal orientation (basal or c-face vs. prism or a-face) or on crystallinity (single-crystal vs. polycrystalline samples). The steady-state sublimation rate is attained just as rapidly as the steady-state temperature.

2) The plot of log J vs. T^{-1} is a curve with a characteristic shape for all ice samples (except those grown from concentrated solutions of NH_4F and NH_4OH). The activation enthalpy of sublimation ΔH_s^* is equal to the equilibrium enthalpy of sublimation ΔH_s° at low temperatures (< 85°) and approaches a limiting value of about $\frac{1}{2}\Delta H_s^\circ$ at high temperatures (> -40°).

3) The surface of freely vaporizing ice is smooth (apart from transient etch pits) in the temperature range for which $\alpha_v = 1$ (< -85°) and becomes increasingly rough in the temperature range (> -85°C) for which α_v decreases progressively from unity.

4) Ionic impurities in ice in very small (ppm) concentrations appear to cause a shift in the characteristic sublimation rate curve (decrease the sublimation rate). The impurities do not have a cumulative effect on the rate and do not appear to collect on the surface.

5) NH_3(gas) impinging on the vaporizing surface causes a reduction in J; HF(gas) impinging on the vaporizing surface causes an increase in J.

The most important feature of the vaporization characteristics of ice is the marked curvature in the plot of log J vs. T^{-1}, implying a large change in the experimental activation enthalpy ΔH_s^* within the temperature range studied (see Figures 2c and 2d). This feature has never before been reported in vaporization rate studies of ice.

It will be noted that at low temperatures $\Delta H_s^* \rightarrow \Delta H_s^\circ$, and for the high-purity samples, $\alpha_v \rightarrow 1$. At high temperature it is more difficult to determine the limiting slope with certainty; rate measurements up to -35° or -30°C would be of great value. An argument will be given below suggesting that the probable high-temperature limiting value for ΔH_s^* is $\frac{1}{2}\Delta H_s^\circ$, as indicated in Figures 3c and 3d.

A change of the activation enthalpy of sublimation indicates a change in the mechanism of sublimation. The observation that at low temperatures the maximum vaporization rate is obtained indicates that under these conditions the vaporizing species are present in their maximum (equilibrium) concentration at the surface and are in equilibrium with the various surface sites. The vaporization rate is thus limited by the desorption of these water molecules. As the temperature is increased the vaporization rate increases rapidly as well, but not as rapidly as J_{max}. It appears that the surface concentration of water molecules that are available for vaporization is no longer large enough to maintain the maximum rate. There is no longer equilibrium between the vaporizing species and the different surface sites. A lower-than-equilibrium surface concentration of vaporizing water molecules would decrease the evaporation rate but would not necessarily give rise to a change in the activation enthalpy of vaporization. Thus, it appears that not only is the surface concentration of vaporizing molecules is changed, but also that the rate-limiting reaction step that controls the vaporization rate has changed from desoprtion of water molecules to some other reaction step.

Proposed mechanism. In order to arrive at a model for the vaporization mechanism of ice we may consider the crystal structure of ice which is shown in Figure 7. Water molecules in ice have at most four nearest

neighbors. It is possible to distinguish between water molecules which have, in turn, 4, 3, 2, and 1 neighboring water molecules.

The model of ice in Figure 7| is small enough so that all but one of the "molecules" are part of a surface: of the 39 molecules represented there are eight molecules with 4 nearest neighbors, twenty-two with 3 nearest neighbors, and nine with 2 nearest neighbors. No molecules with only 1 nearest neighbor are shown, but they may be imagined as admolecules on one of the surfaces. For ease in referring to the various species, a molecule with n nearest neighbors will be called "n-bonded".

A smooth low-index ice surface contains equal numbers of 4-bonded and 3-bonded molecules; a ledge will necessarily have a large number of 2-bonded molecules. A rough surface is one with many ledges and it is not unreasonable to assume that the number of 2-bonded water molecules on a rough surface should be of the same magnitude as the number of 3-bonded and 4-bonded.

We now make the following assumptions:
In the temperature range of interest,
1)/ the oxygen sublattice extends to the surface without major rearrangement.

2) The positions of the hydrogens do not need to be considered as they are randomly arranged.

3) 2-bonded water molecules are present on the surface of freely vaporizing ice in a concentration $[W_2]$ that is of the same magnitude as the concentration of 3-bonded and 4-bonded water molecules. Because $[W_2]$ is so large, it does not change markedly with temperature. This assumption may not be justified for low temperatures at which $\alpha_v \lesssim 1$,

but as will be shown the vaporization rate is not very dependent on $[W_2]$ in this temperature region. It is worthwhile to point out that vaporization is not expected to alter the population of 3-bonded and 2-bonded molecules because they are replenished at the same average rate at which they are used up.

4) Molecules with only one neighbor are uniformly distributed over the ice surface. These admolecules are also most likely the high-surface-mobility species responsible for sintering. (Murphy has proposed that these molecules might owe their mobility to a kind of "bipedal random walk" in which a molecule is alternately 1-bonded and 2-bonded as it moves across the ice surface.) They are presumably considerably more mobile than the molecules with 2, 3 or 4 neighbors. At the temperatures included in the present study, their concentration $[W_1]$ will be small compared to the total number of molecules on the surface ($[W_1] \ll 10^{15} cm^2$).

The proposed vaporization mechanism is

$$W_2 \underset{k_{12}}{\overset{k_{21}}{\rightleftharpoons}} W_1 \xrightarrow{k_{10}} W_0$$

where W_2 and W_1 are the 2- and 1-bonded water molecules on the ice surface and W_0 is the water vapor molecule. The notation k_{ij} denotes the rate constants for the reaction from state i to state j. In each step one hydrogen bond is broken or re-established; k_{21} and k_{10} include the activation energy to break one bond. It is customary to assume that k_{12} is proportional to the ledge concentration,[1] which for the ice surface varies as $[W_2]$.

The above representation for this surface reaction is formally identical to that for the unimolecular gas-phase decomposition treated in kinetics texts.[36] By assuming the steady-state condition $d[W_1]/dt = 0$, the vaporization rate J can be written

$$J = \frac{k_{10}k_{21}\,W_2}{k_{10} + k_{12}} \quad .$$

In the low-temperature limit, $k_{10} \ll k_{12}$, due to the exponential temperature dependence of k_{10}. In this circumstance the desorption rate of W_1 admolecules limits the vaporization rate. There is a virtual equilibrium of all species on the ice surface for vaporization does not occur rapidly enough to disturb the equilibrium populations. We find this condition to be satisfied below -85°. Note that because k_{12} is proportional to $[W_2]$ and k_{21} and k_{10} each include the activation energy of breaking one hydrogen bond, the prediction of this model is that the low-temperature vaporization rate will be independent of surface roughness and that the activation enthalpy $\Delta H_s^* = \Delta H_s^\circ$.

In the high-temperature limit $k_{10} \gg k_{21}$ and the rate equation reduces to $J = k_{21}[W_2]$. There is a virtual depletion of 1-bonded molecules, for they vaporize as rapidly as they form, at a rate proportional to the surface roughness. Since reaction steps occurring after the rate-limiting step do not influence the kinetics of the reaction, the activation energy reflects only the energy necessary to produce W_1 (that is, the breaking of one hydrogen bond) and not the energy necessary for its subsequent desorption. The model therefore predicts for high temperatures that $\Delta H_s^* \simeq \frac{1}{2}\Delta H_s^o$. We find this condition to be approached at temperatures near -40°. This high-temperature picture of depletion of mobile species is corroborated by the severe retardation of ice sintering in dry atmospheres.[15]

Impurity Effects. The effects of NH_3 (g) and HF (gas) in lowering and raising the vaporization rate of ice at both low and high temperatures are further evidence that breaking of hydrogen bonds i the rate limiting step in the sublimation process. As pointed out previously, each NH_3 or HF molecule that is

incorporated into the ice lattice produces a D or L defect, respectively. The orientational defect concentration is most likely too small compared to the number of vaporizing water molecules at the surface, in pure or even in doped ice samples, to have any detectable effect on the sublimation rate. If the same condition prevails at the ice surface, each NH_3 molecule produces a D-defect and each HF molecule an L-defect. However, the gas fluxes used in these experiments were of the order of magnitude of the ice vaporization rates. Thus, the concentration of adsorbed gas molecules is much larger than their surface concentration that could be established by doping, and so the adsorption of these gas molecules at the vaporizing surface could markedly influence the sublimation rates if the L or D-defects at the surface play a role in the vaporization of ice. If only L-defects have a direct influence on the rate HF should be expected to increase the evaporation rate as it introduces L-defects. Since it seems unlikely that D-defects should themselves decrease the vaporization rate, the rate reducing influence of adsorbed NH_3 would be to decrease the surface L-defect concentration below the level for pure ice, in a manner similar to that described by Jones and Glen.[25] It should be noted that the activation energy to form an L-defect is likely to be about the same as the energy required to break a hydrogen bond.

The effect of these gases may also be viewed as being due to their differing number of protons as compared to H_2O in the lattice. The excess hydrogen in NH_3 and the hydrogen deficiency in HF could shift the equilibria between the surface species, W_1 and W_2, if these molecules enter the ice lattice substitutionally. It is not possible at present to consider the effect of adsorbed NH_3 and HF on the vaporization of ice in more detail since the surface concentration of Bjerrum defects is unknown and

the specific nature of the chemical interactions of gaseous NH_3 and HF with the surface has not been investigated.

The role of impurities other than NH_3 and HF on the properties of ice has not been as extensively studied. Kelley and Salomon[24] show that the dielectric relaxation time decreases and the activation energy increases with increasing concentrations of NaOH in the ice lattice. This observation is consistent with a general increase in lattice binding energy atrributable to long-range ionic interactions. On the other hand, NH_4F causes a large decrease in the dielectric relaxation activation energy. Causes for this effect have been proposed but remain uncertain.[23]

The shape of the vaporization curve for ice samples doped with various impurities indicates that at low temperatures ΔH_s^* is still equal to ΔH_s°, i.e., doping does not change the slope. Equilibrium between W_2 and W_1 surface species is maintained but shifted towards W_2. Doping thus appears to cause a reduction in the equilibrium population of W_1 on the vaporizing ice surface and consequently a reduction in the vaporization rate at temperatures for which desorption of W_1 molecules is the rate-determining step. Because the doping levels attainable were low and non-uniform it is difficult to draw firm conclusions about the exact role of impurities in the ice lattice on the sublimation rates.

It seems likely that the fluctuations in the observed rate for the undoped samples are due to an uncontrolled incorporation of trace amounts of impurity in the samples during growth. (The magnitude of the fluctuation-- $\pm$ 50 $\mu g\ cm^{-2} min^{-1}$-- is unimportant when compared to vaporization rates above about -75°C but it did make it difficult to collect reliable data below that temperature.) The magnitude of the fluctuation was reduced

at least tenfold, both by growing samples of higher purity and by deliberate doping. If the high rate fluctuations for the undoped samples are due to local variations in the type and concentration of impurities, then either an overall reduction in the impurity concentration or moderate doping with one type of impurity would serve to suppress this effect.

The results for ice doped with NH_4F may be discussed separately. As mentioned above, the solubility of NH_4F in ice is appreciable, and it is likely (although no measurements were made) that the concentration of NH_4F in the ice samples whose rate is shown in Figure 4 is only a factor of 10 lower than the solution concentrations given.[23] Since HF(gas) has been observed to raise the vaporization rate and NH_3(gas) to lower it, it appears that when they are both present in the ice lattice in an associated form as NH_4F their effect is markedly different from the effects of the dissociated molecules. this result is to be expected, however, since ammonium fluoride is likely to be present in the ice lattice as ion pairs NH_4^+-F^- and not as neutral molecules.[23]

It is important to note that for all of the impurities investigated there was no apparent tendency for them to build up on the surface and reduce the rate as vaporization progressed by permanent blocking of surface sites. This observation is corroborated by electron micrography of an ice single crystal grown from a 0.01M solution of NH_4F and vaporized 1 min. at -100°C. The surface appeared quite similar to the surface of a similar oriented pure ice single crystal after the same vaporization.

Extrapolation of the vaporization rate to the melting point of ice (assuming an activation enthalpy of vaporization of $\Delta H^* = \frac{1}{2}\Delta H_s^\circ$) yields an

evaporation coefficient $\alpha_v(0°C) \approx 0.07$. This value is not much higher than the values reported by Delaney et al.[5] (see Figure 1). It is interesting to speculate whether melting will change the mechanism of vaporization. Recent studies of the vaporization of organic liquids (glycerin, triethylene glycol) where hydrogen bonding predominates the intermolecular interaction indicate that the breaking of hydrogen bonds is also the likely rate-determining step in their vaporization and $\alpha_v < 1$.

ACKNOWLEDGMENT

This work was performed under the auspices of the United Stated Atomic Energy Commision. We are grateful to F. R. McFeely for the use of unpublished results of vaporization rates of organic liquids.

FIGURE CAPTIONS

Figure 1. Ice Vaporization Rates by Different Investigators.

Figure 2a. Scheme of Microbalance Vacuum Chamber.

Figure 2b. Heat Flow Model.

Figure 3. Vaporization Rates of Undoped and High-Purity Ice.

Figure 4. Vaporization Rates of Ice Grown from Various Solutions of NH_4F.

Figure 5. Effect of a)Gas Pressure and b)Sample Temperature on the Vaporization Rate of Pure Ice.

Figure 6. Predicted limiting behavior of ice vaporization rate for $\alpha_v = 1$ with decrease in mean free path.

Figure 7. The Crystal Structure of Ice.

TABLE CAPTION

TABLE 1. The Evaporation Coefficient, α_v at -65°C for Single Crystals Grown from Solution by the Jona-Scherrer Method.

TABLE I

The Evaporation Coefficient, α_v at -65°C for Single Crystals Grown from Solution by the Jona-Scherer Method.

Dopant	α_v (at -65°C) Solution Concentration 0.01M	0.1M
NH_4OH	.80, .60	.64
LiOH	.73	.71
NaOH	.86	.87
HF	.77, .73	
HNO_3		.78
NH_4F	.64	.40, .29
LiF	.73	.78
NaF	.80	.47, .54

REFERENCES

1. G. A. Somorjai and J. E. Lester, Progr. Solid State Chem. 4, 1 (1967).
2. D. Eisenberg and W. Kauzmann, The Structure and Properties of Water (Oxford University Press, 1969), pp. 47, 100.
3. G. Jancso, et al., J. Phys. Chem. 74, 2984 (1970).
4. R. J. List, Smithsonian Meteorological Tables, vol. 114 (Smithsonian Institution, Washington D.C., 1951), p. 350.
5. L. J. Delaney et al., Chem. Eng. Sci. 19, 105 (1964).
6. M. K. Baranaev, Zhur. Phyz. Chim. 20, 399 (1946). (In Russian)
7. T. Alty, Proc. Roy. Soc. 161, 68 (1937).
8. R. J. Strickland-Constable and E. W. Bruce, Trans. Instr. Chem. Engrs. 32, 192 (1954).
9. H. Kramers and S. Stemerding, Appl. Sci. Res. A3, 73 (1951).
10. K. Tschudin, Helv. Phys. Acta. 19, 91 (1946). (In German)
11. R. M. Koros et al., Chem. Eng. Sci. 21, 941 (1966).
12. K. Isono and K. Iwai, Nature 223, 1149 (1969).
13. T. A. Milne and F. T. Greene, J. Chem. Phys. 47, 3668 (1967).
14. F. T. Greene, et al., 1969 Midwest Research Institute Summary Technical Report, 27 June 1967-31 July 1969.
15. H. H. G. Jellinek, J. Colloid and Interface Sci. 25, 192 (1967).
16. J. G. Davy and D. Branton, Science 168, 1216 (1970).
17. J. D. Bernal, ed., A Discussion on the Physics of Water and Ice, a collection of 12 papers published as Proc. Roy. Soc. A247, No. 1251, 1968; B. J. Mason, ed., The Physics of Water and Ice, a collection of 8 papers published as Advances in Physics (Quarterly Supplement to Phil. Mag.) 7, No. 26, 1958.
18. F. A. Kröger, The Chemistry of Imperfect Crystals (North-Holland, Amsterdam, 1964), pp. 750-760.
19. W. W. Webb and C. E. Hayes, Phil. Mag. 16, 909 (1967).
20. A. Fukuda and A. Higashi, Jap. J. Appl. Phys. 8, 993 (1969).
21. J. E. Lester and G. A. Somorjai, J. Chem. Phys. 49, 2940 (1968).
22. A. Von Hippel et al., J. Chem. Phys. 54, 134, 145, 150 (1971).

23. G. W. Gross, in Trace Inorganics in Water (American Chemical Society Advances in Chemistry Series) vol. 73, p. 27, 1968.

24. J. G. Young and R. E. Salomon, J. Chem. Phys. 48, 1635 (1968); D. J. Kelley and R. E. Salomon, ibid., 50, 75 (1969).

25. S. J. Jones and J. W. Glen, Phil. Mag. 19, 13 (1969).

26. L. Onsager and L. K. Runnels, J. Chem. Phys. 50, 1089 (1969).

27. F. Jona and P. Scherrer, Helv. Phys. Acta. 25, 35 (1952) (in German). For a discussion in English, see R. Siksna, Arkiv for Fysik 11, 495 (1957).

28. E. Wood, Crystals and Light, p. 94. Princeton, N. J: D. Van Nostrand Co., Inc., 1964.)

29. L. C. Labowitz and E. F. Westrum, Jr., J. Phys. Chem. 65, 408 (1961).

30. C. Jaccard and L. Levi, Z. Angewandte Math u. Physik 7, 70 (1961) (in French).

31. J. G. Davy, in Vacuum Microbalance Techniques, Vol. 8 (Plenum Press, New York, 1971).

32. H. W. Melville, Trans. Faraday Soc. 32, 1017 (1936).

33. L. Brewer and J. S. Kane, J. Phys. Chem. 59, 105 (1955).

34. G. M. Rosenblatt, J. Electrochem. Soc. 110, 563 (1963).

35. G. Burrows, Trans. Instr. Chem. Engrs. 32, 23 (1954); J. Appl. Chem. 7, 375 (1957).

36. Frost and Pearson, Kinetics and Mechanism (Wiley, New York, 1961), p. 70.

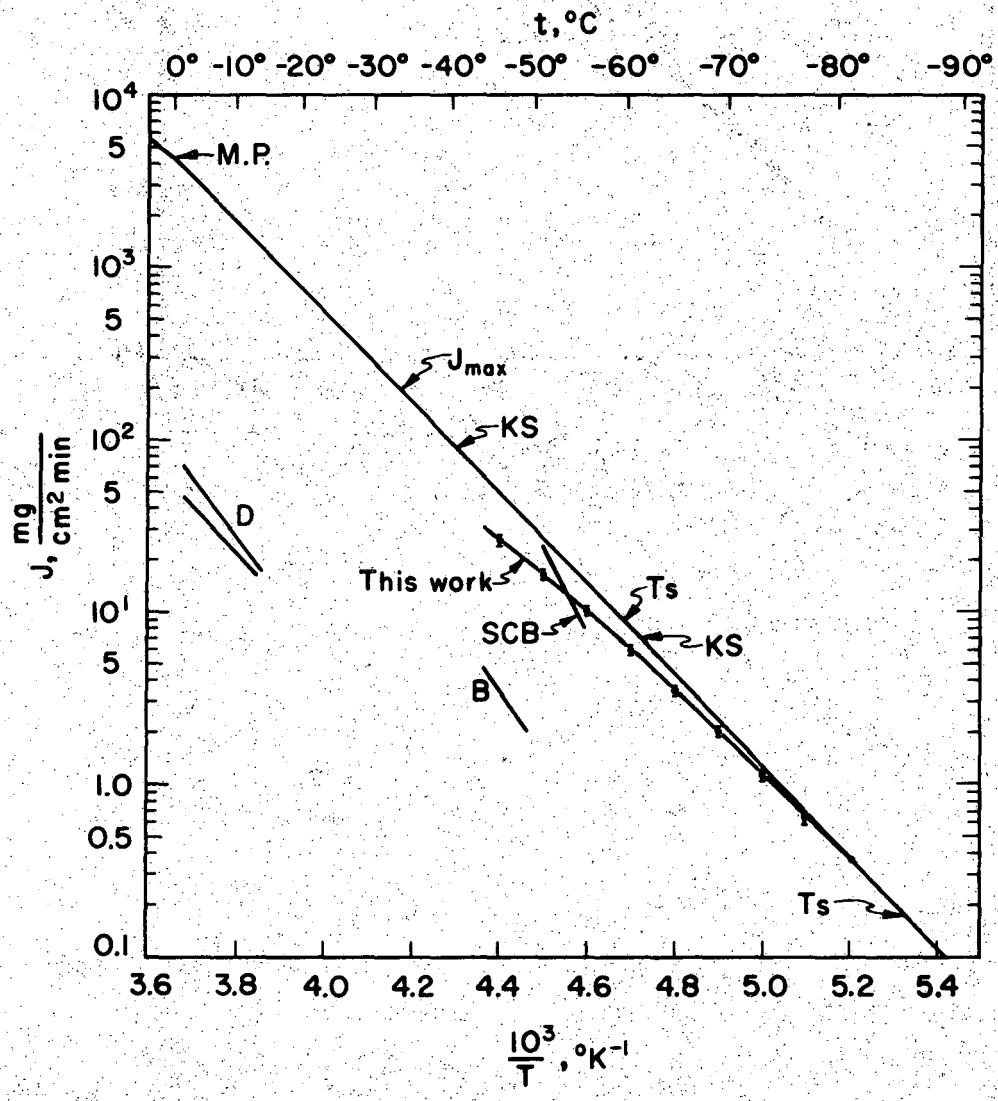
t, °C
0° -10° -20° -30° -40° -50° -60° -70° -80° -90°
10^4
5
10^3
5
10^2
5
10^1
5
1.0
0.5
0.1
M.P.
J_{max}
KS
D
This work
Ts
SCB
KS
B
Ts
$\frac{mg}{J, cm^2 min}$
3.6 3.8 4.0 4.2 4.4 4.6 4.8 5.0 5.2 5.4
$\frac{10^3}{T}$, °K^{-1}
XBL 713-6570

Fig.1

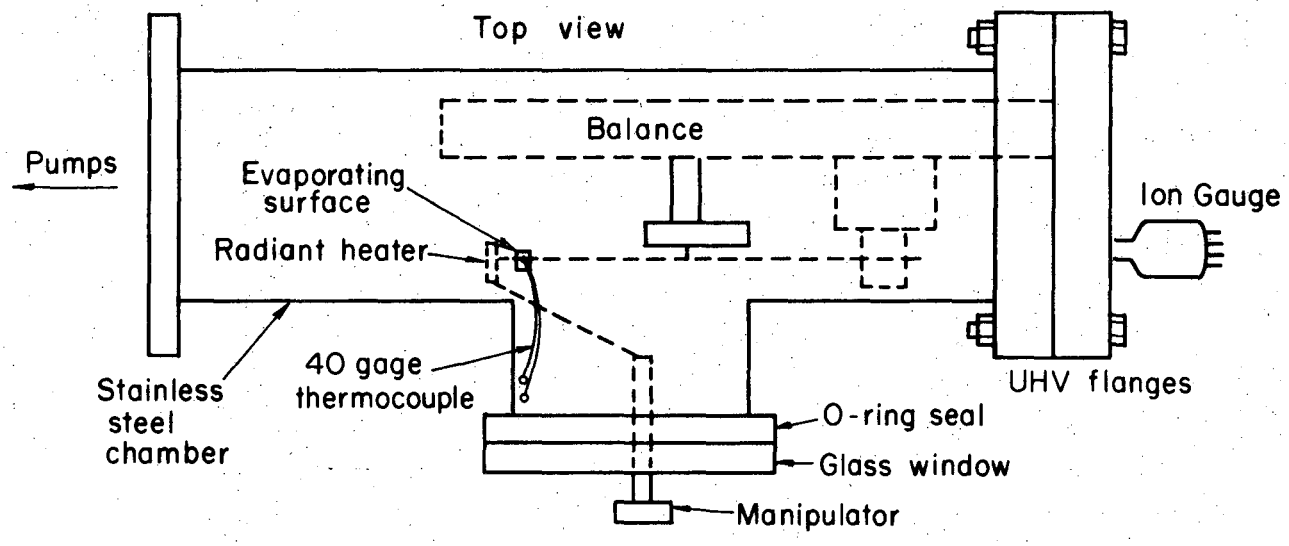

XBL712-6567

Fig.2a

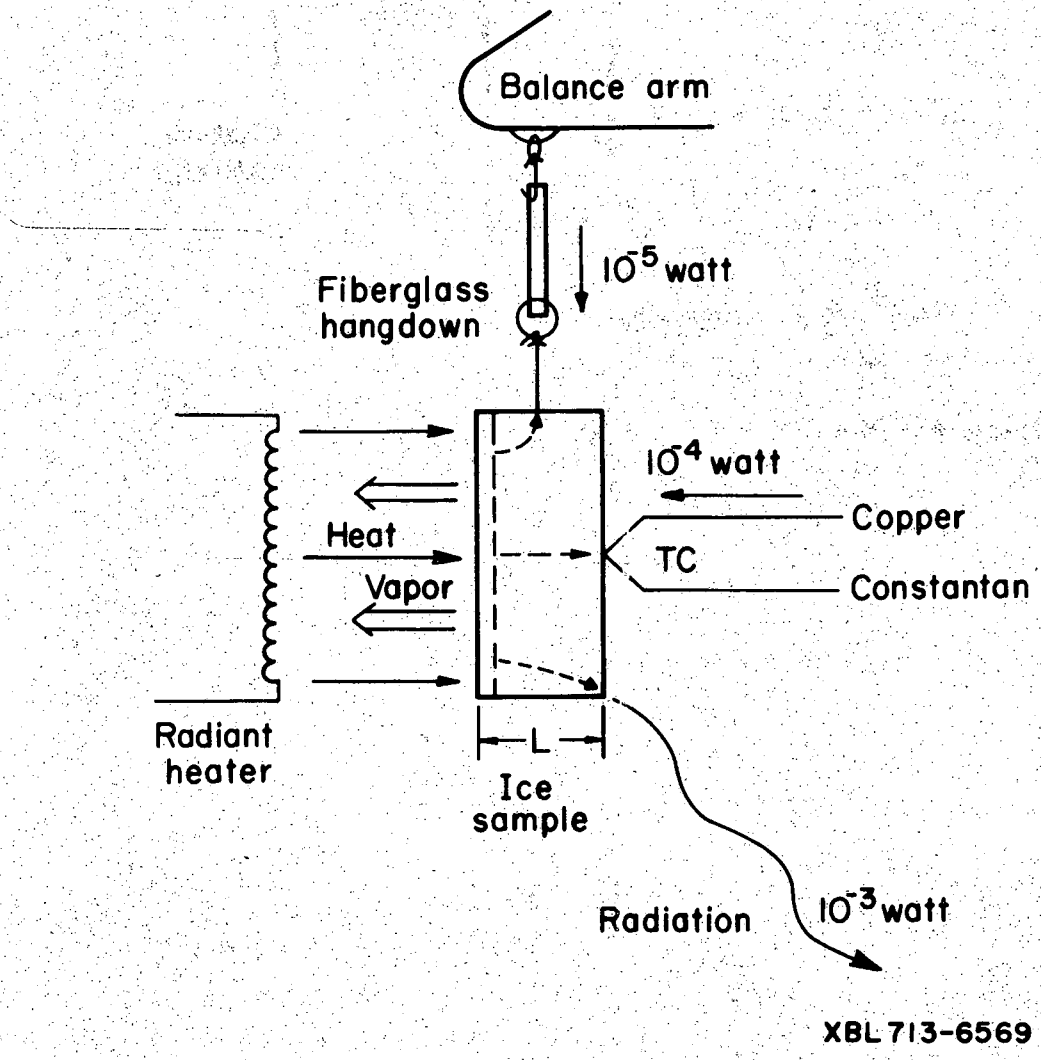
Balance arm
10^{-5} watt
Fiberglass hangdown
10^{-4} watt
Copper
Heat
TC
Vapor
Constantan
Radiant heater
L
Ice sample
Radiation
10^{-3} watt
XBL 713-6569

Fig. 2b

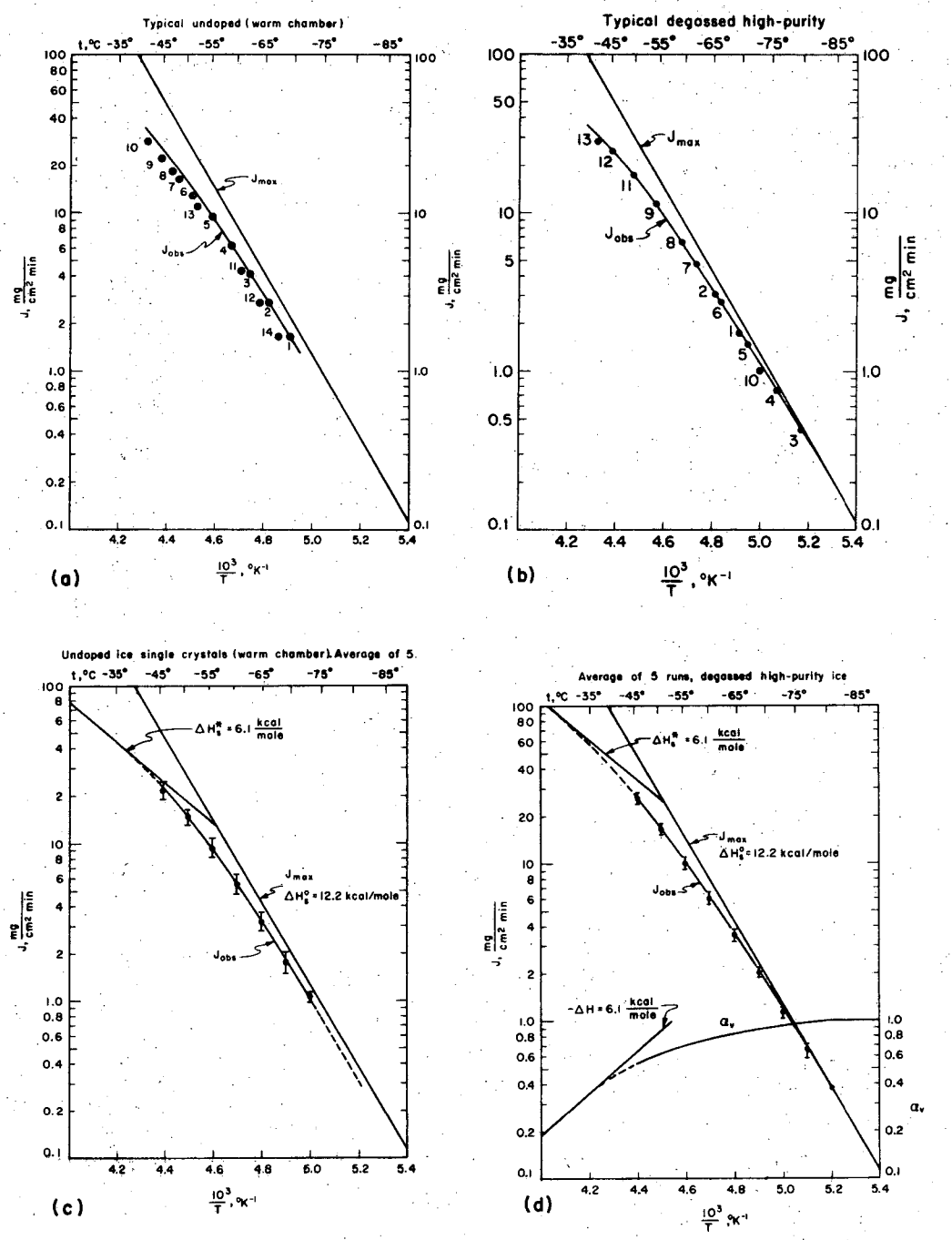
Typical undoped (warm chamber)
Typical degassed high-purity
Undoped ice single crystals (warm chamber). Average of 5.
Average of 5 runs, degassed high-purity ice
t, °C -35° -45° -55° -65° -75° -85°
J_{max}
J_{obs}
$\Delta H_s^o = 6.1 \frac{kcal}{mole}$
$\Delta H_s^o = 12.2$ kcal/mole
$-\Delta H = 6.1 \frac{kcal}{mole}$
α_v
$\frac{mg}{J, cm^2 min}$
$\frac{10^3}{T}, °K^{-1}$
(a)
(b)
(c)
(d)
XBL 713-6571

Fig. 3

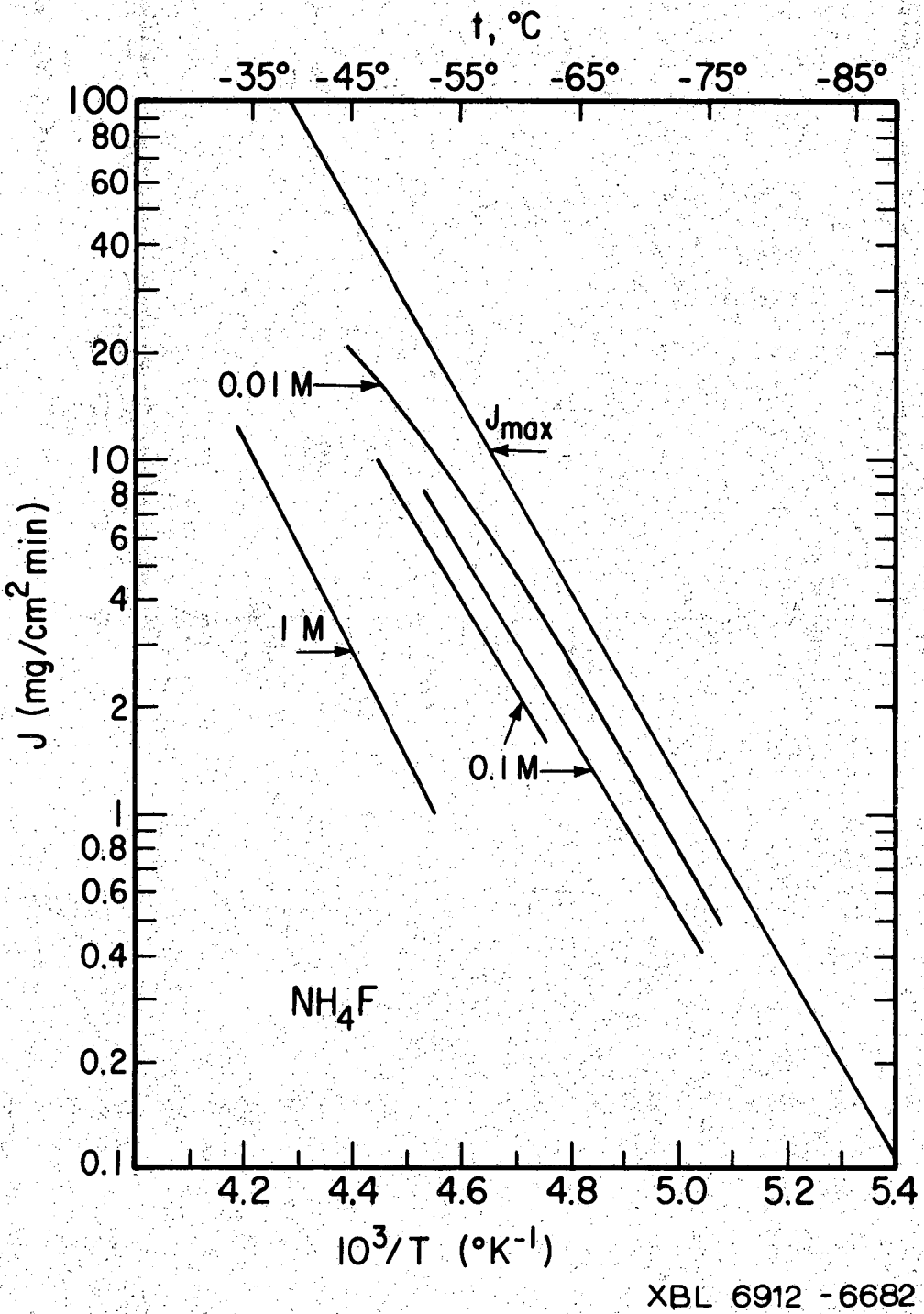
t, °C
-35°
-45°
-55°
-65°
-75°
-85°
100
80
60
40
20
10
8
6
4
2
1
0.8
0.6
0.4
0.2
0.1
J (mg/cm² min)
0.01 M
J max
1 M
0.1 M
NH4F
4.2
4.4
4.6
4.8
5.0
5.2
5.4
10³/T (°K⁻¹)
XBL 6912 -6682

Fig. 4

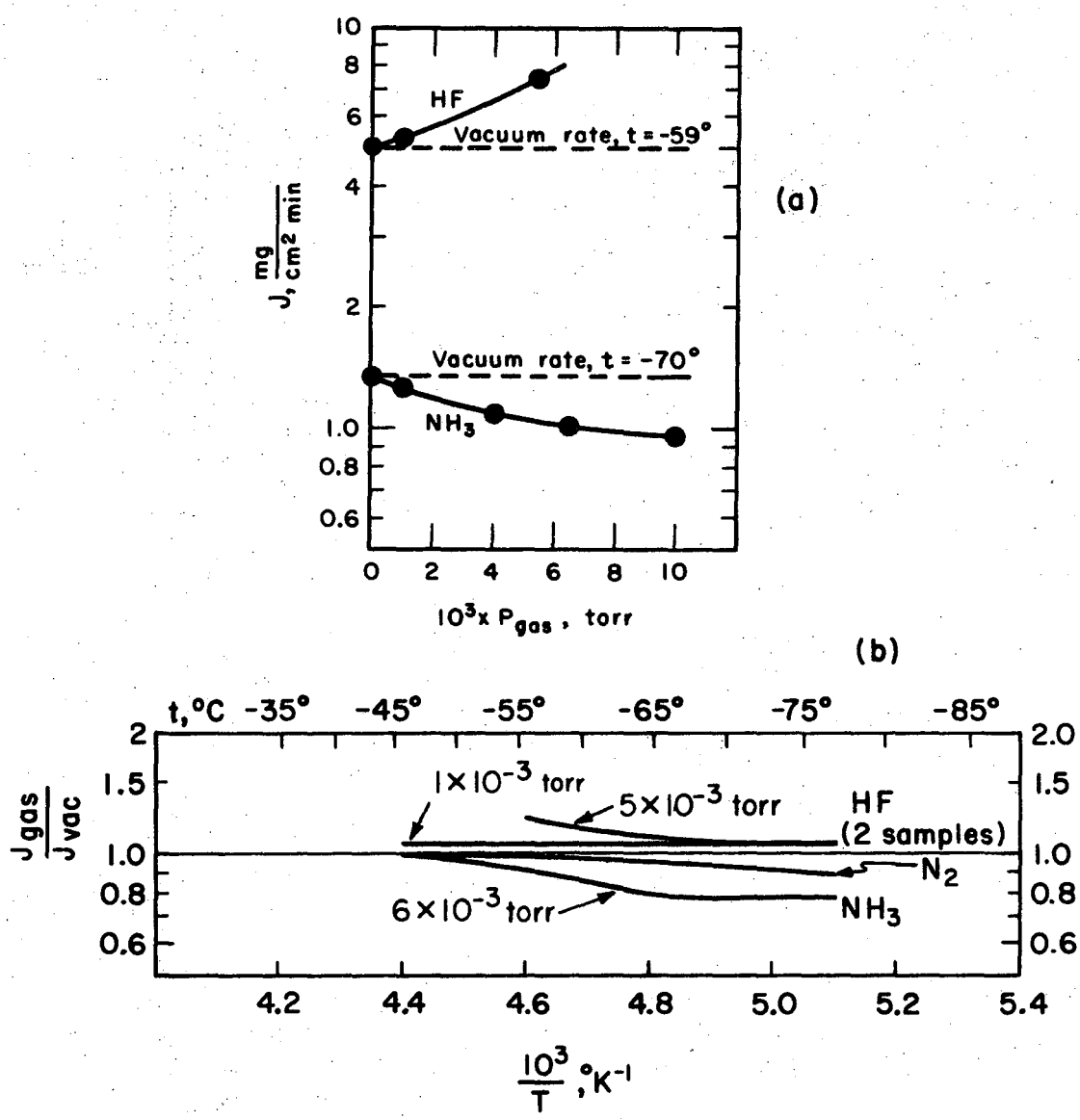
(a)
HF
Vacuum rate, t = -59°
Vacuum rate, t = -70°
NH3
mg / J, cm² min
10
8
6
4
2
1.0
0.8
0.6
0
2
4
6
8
10
10³x P gas , torr
(b)
t,°C -35° -45° -55° -65° -75° -85°
Jgas / Jvac
1×10⁻³ torr
5×10⁻³ torr
HF
(2 samples)
N2
6×10⁻³ torr
NH3
2
1.5
1.0
0.8
0.6
2.0
1.5
1.0
0.8
0.6
4.2
4.4
4.6
4.8
5.0
5.2
5.4
10³ / T , °K⁻¹
XBL713-6572

Fig. 5

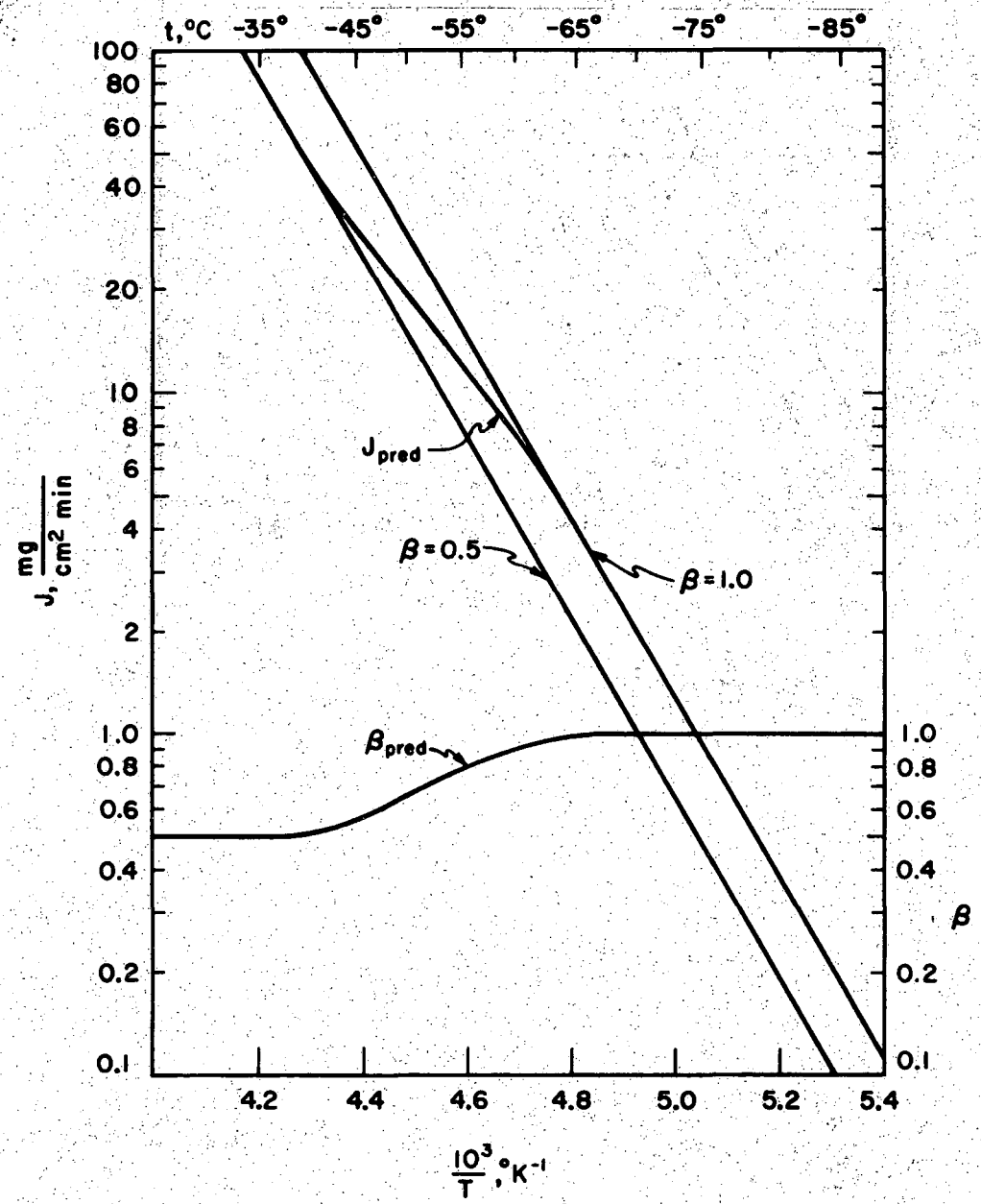
t,°C -35° -45° -55° -65° -75° -85°
100
80
60
40
20
10
8
6
4
2
1.0
0.8
0.6
0.4
0.2
0.1
J, mg/cm² min
J_pred
β = 0.5
β = 1.0
β_pred
β
4.2 4.4 4.6 4.8 5.0 5.2 5.4
10³/T, °K⁻¹
XBL6911-6167

Fig. 6

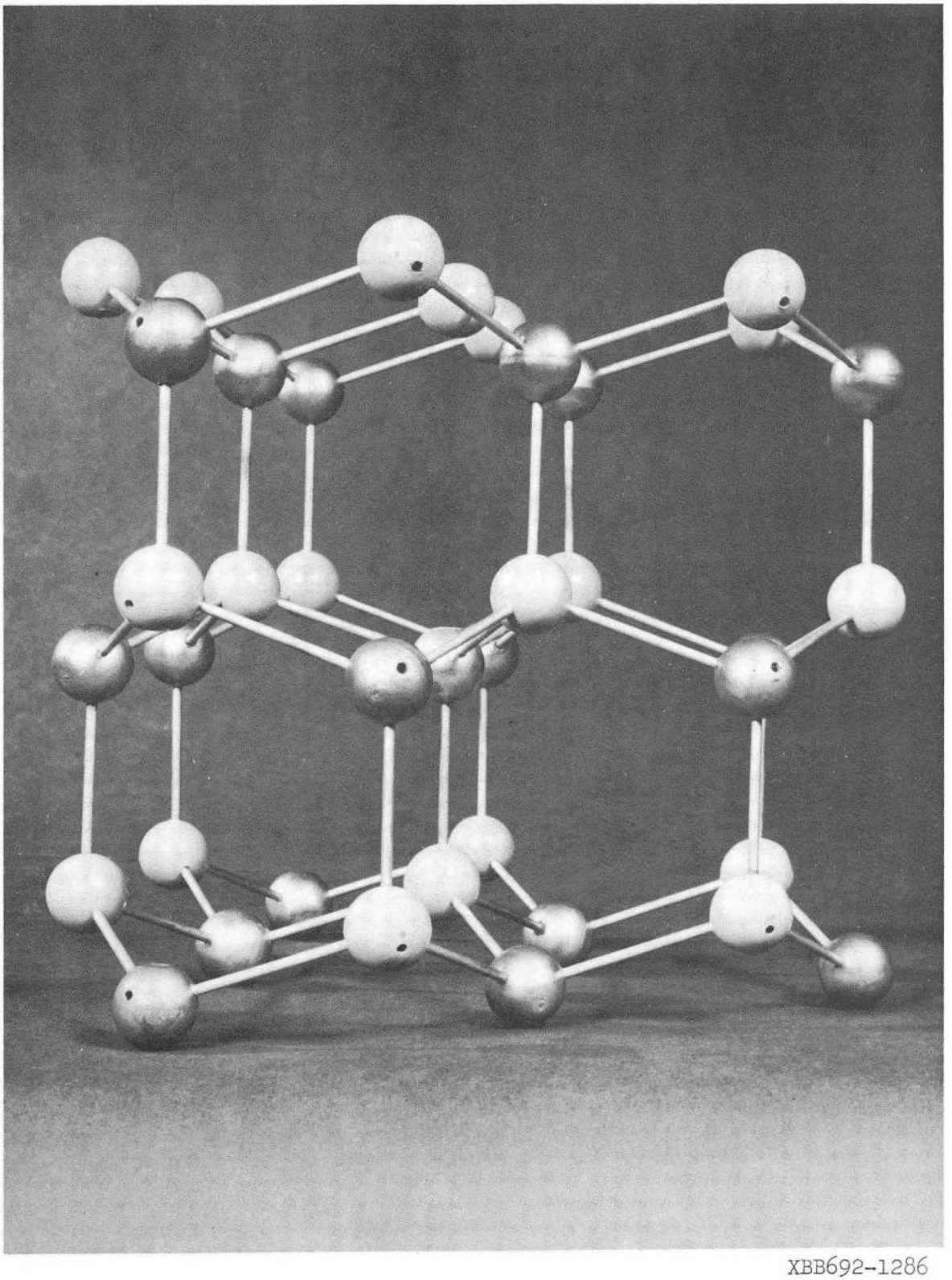

XBB692-1286

Fig. 7

TECHNICAL INFORMATION DIVISION
LAWRENCE RADIATION LABORATORY
UNIVERSITY OF CALIFORNIA
BERKELEY, CALIFORNIA 94720